

# Three-Dimensional Ignition and Flame Propagation Above Liquid Fuel Pools: Computational Analysis

Jinsheng Cai, Feng Liu, and William A. Sirignano

*Department of Mechanical and Aerospace Engineering  
University of California, Irvine, CA 92697-3975*

**Abstract:** A three-dimensional unsteady reactive Navier-Stokes code is developed to study the ignition and flame spread above liquid fuels initially below the flashpoint temperature. Opposed air flow to the flame spread due to forced and/or natural convection is considered. Pools of finite width and length are studied in air channels of prescribed height and width. Three-dimensional effects of the flame front near the edge of the pool are captured in the computation. The formation of a recirculation zone in the gas phase similar to that found in two-dimensional calculations is also present in the three-dimensional calculations. Both uniform spread and pulsating spread modes are found in the calculated results.

**Introduction:** Schiller, Ross, and Sirignano [1] studied ignition and flame spread above liquid fuels initially below the flashpoint temperature by using a two-dimensional computational fluid dynamics code that solves the coupled equations of both the gas and the liquid phases. Their computational studies and analysis identified the mechanisms for uniform and pulsating flame spread and studied the effects of gravity level, pool depth, fluid properties, and chemical kinetic coefficients on flame spread across liquid fuel pools. Pulsating flame spread was attributed to the establishment of a gas-phase recirculation cell that forms just ahead of the flame leading edge because of the opposing effect of buoyancy-driven flow in the gas phase and the thermocapillary-driven flow in the liquid phase. Schiller and Sirignano [2] extended the same study to include flame spread with forced opposed flow in the gas phase. A transition opposed flow velocity was found above which an originally uniform spreading flame becomes pulsating. The same type of gas-phase recirculation cell caused by the combination of forced opposed flow, buoyancy-driven flow, and thermocapillary-driven concurrent flow was found to be responsible for the pulsating flame spread. Ross and Miller [3] and Miller and Ross [4] performed experimental work that generally corroborate many of the computational findings in References 1 and 2.

In this paper, we extend previous two-dimensional and axisymmetric studies in References 1, 2, and 5 to three-dimensions. Figure 1 shows the geometry of the three-dimensional model. The mathematical formulation of the problem and assumptions are the same as those in References 2.

**Results and Discussion:** Ten cases at five different initial temperature  $T_0$  under both normal gravity and zero gravity are studied:  $T_0 = 17^\circ\text{C}$ ,  $19^\circ\text{C}$ ,  $21^\circ\text{C}$ ,  $23^\circ\text{C}$ , and  $25^\circ\text{C}$ . The mean flow velocity at the entrance of the wind tunnel is fixed at 30 cm/s for these cases.

Figure 2 shows the contours of fuel consumption rate at normal gravity 0.22 seconds after ignition in the  $x$ - $y$  symmetry plane at  $z/L = 0.0$  for  $T = 21^\circ\text{C}$ . Figure 3 shows contours of temperature and flow velocity vectors relative to the flame in the same plane. The spatial coordinates presented here are non-dimensionalized by the total length of the wind-tunnel, i.e., 36 cm. Near the surface of the liquid pool, surface tension pulls the fluid forward ahead of the flame while the forced flow velocity goes against this motion. This causes a small vortex cell in front of the flame as shown by the velocity vectors in Figure 3. A top view of the flame ( $x - z$ ) plane at a dimensionless distance of  $y/L = 0.00277$  from the liquid fuel surface is shown in Figure 4. The flame at the corner curves around and continues along the edge of the fuel pool. Figure 5 shows the contours of fuel consumption rate in a cross-section at  $x/L = 0.805$ . The flame extends beyond the fuel pool and attaches to the wind-tunnel floor by the pool edge. Figure 6 plots the velocity vectors and contours of temperature in the same plane. Buoyancy effects pull the flow into the flame from the side very near the wind tunnel floor and close to the flame whereas the flow expands out from the pool away from the wind-tunnel wall. Thermal expansion and buoyancy effects create a streamwise vortex near the two edges of the liquid pool. Despite the three-dimensional effects, computations show that the basic features of the flame propagation process is the same as those in the two-dimensional simulations. The formation of a recirculation zone in the gas phase is necessary for pulsating spread of the flame. Further studies will include more detailed simulation of the propagation of the flame over the whole pool surface and also variation of parameters such as forced flow speed, initial temperature, liquid pool width and depth.

Figure 7 shows the calculated history of the flame position, here defined as the maximum fuel consumption rate location, in the  $x$ - $y$  symmetry plane for all ten cases within the computed time period. As initial fuel temperature increases, the mean flame speed increases while the size of the recirculation zone and the period of pulsation decrease. At the lower temperature of  $17^\circ\text{C}$  to  $21^\circ\text{C}$ , the flame propagates in a pulsating mode under both normal and zero gravity levels. The mean flame speed at normal gravity is greater than the flame speed at zero gravity. At  $23^\circ\text{C}$ , the flame under zero gravity starts to propagate with a uniform speed while the flame under normal gravity still moves in a pulsating mode. The flame speed under zero gravity is faster than that under normal gravity. When the initial temperature is further increased to  $25^\circ\text{C}$ , both flames under normal and zero gravity spread uniformly and there is negligible difference in speed.

The three-dimensional code produced two-dimensional results when the normal gradients at the lateral boundaries were set to zero and the initial conditions were two-dimensional. The two-dimensional results for mean flame speed was very similar to the three-dimensional results.

**Acknowledgments:** This research was conducted in support of NASA Grant No. NAG3-2024 under the technical monitoring of Dr. Howard Ross. Computer time was provided by the San Diego Supercomputer Center, the NASA Center for Computational Sciences, and the UCI Office of Academic Computing.

# References

- [1] D. N. Schiller, H. D. Ross, and W. A. Sirignano. Computational analysis of flame spread over alcohol pools. *Combustion Science and Technology*, 118(4-6):205–258, May 1996.
- [2] D. N. Schiller and W. A. Sirignano. Opposed-flow flame spread across n-propanol pools. In *Proceedings of the Twenty-Sixth International Symposium on Combustion*, pages 1319–1325, 1996.
- [3] Howard D. Ross and Fletcher J. Miller. Flame spread across liquid pools with very low-speed opposed or concurrent airflow. In *Proceedings of the Twenty-Seventh International Symposium on Combustion*, pages 2723–2729, 1998.
- [4] Fletcher J. Miller and Howard D. Ross. Smoke visualization of the gas-phase flow during flame spread across a liquid pool. In *Proceedings of the Twenty-Seventh International Symposium on Combustion*, pages 2715–2722, 1998.
- [5] I. Kim, D. N. Schiller, and W. A. Sirignano. Axisymmetric flame spread across propanol pools in normal and zero gravities. *Combustion Science and Technology*, 139(1-6):249, 1999.

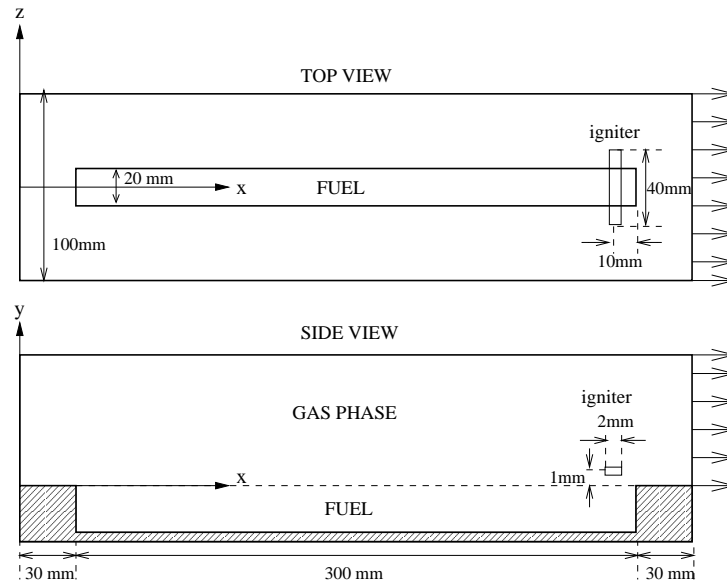


Figure 1: Geometry for the three-dimensional liquid fuel pool in a wind-tunnel with forced flow

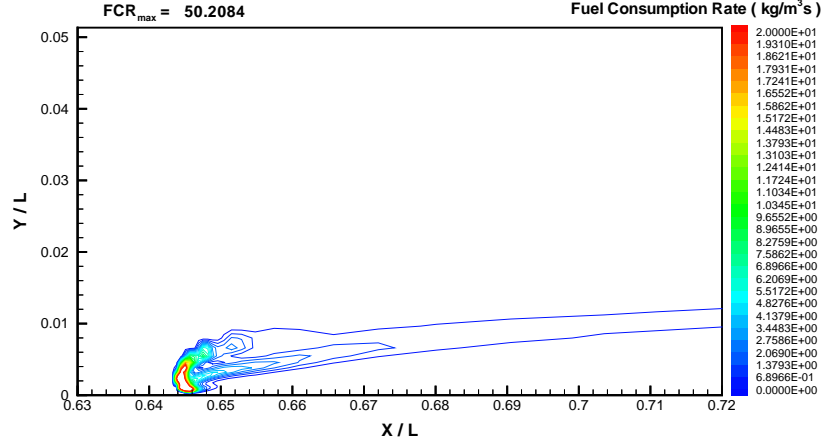


Figure 2: Contours of fuel consumption rate in the  $x$ - $y$  symmetry plane ( $z/L = 0.0$ ),  $t = 2.2s$ , normal gravity.

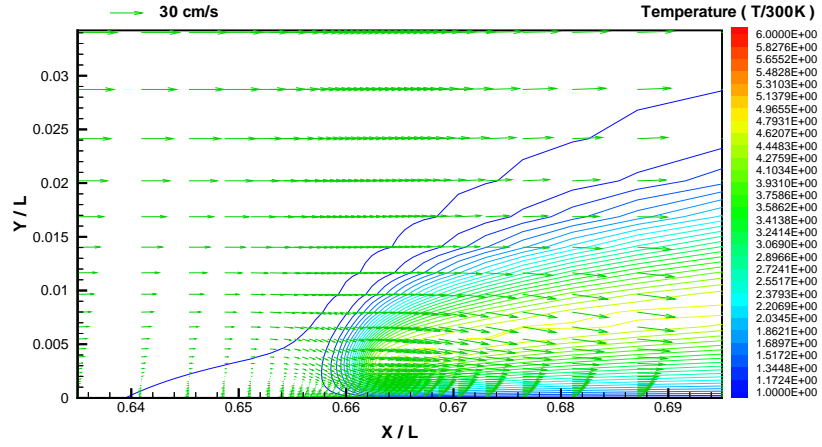


Figure 3: Relative velocity vectors and contours of temperature in the  $x$ - $y$  symmetry plane ( $z/L = 0.0$ ),  $t = 2.2s$ , normal gravity.

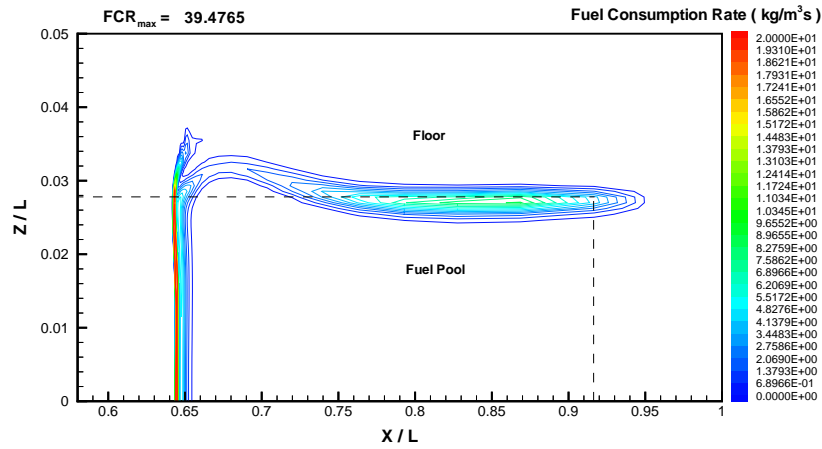


Figure 4: Top view of contours of fuel consumption rate in the  $x$ - $z$  plane at  $y/L = 0.00277$ ,  $t = 2.2$ , normal gravity.

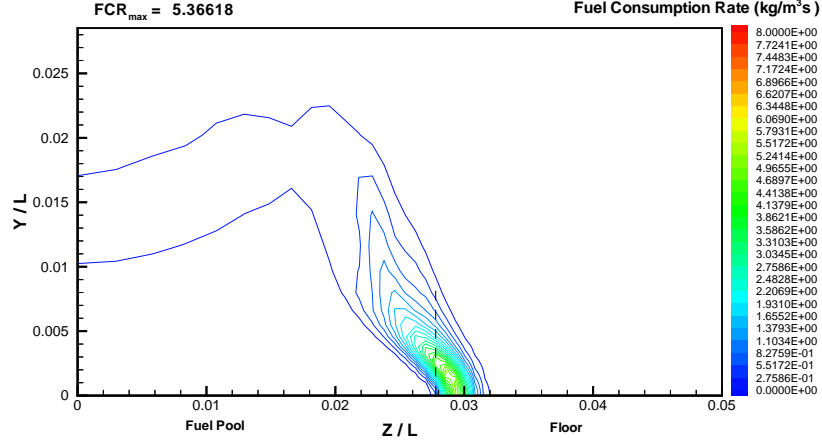


Figure 5: Rear view of contours of fuel consumption rate in the  $y$ - $z$  plane at  $x/L = 0.75$ ,  $t = 2.2$ , normal gravity.

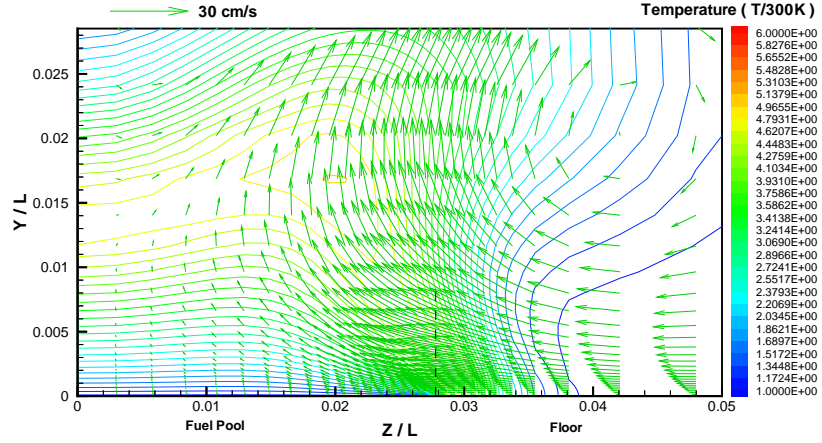


Figure 6: Rear view of velocity vectors and contours of temperature in the  $y$ - $z$  plane at  $x/L = 0.75$ ,  $t = 2.2$ , normal gravity.

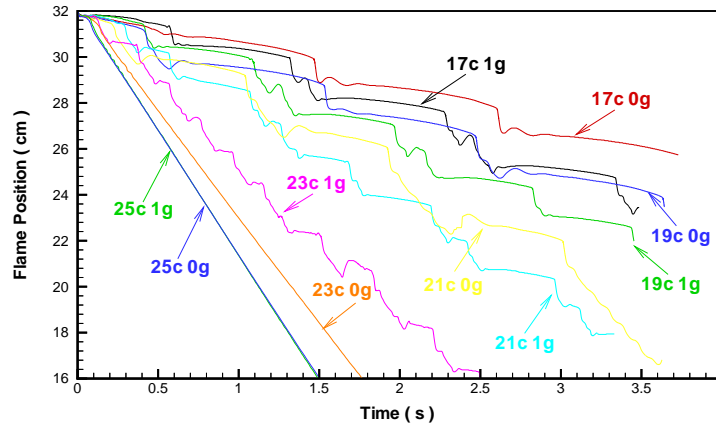


Figure 7: Flame position in the symmetry plane vs. time.